

Journal of
Mechanics of
Materials and Structures

**RECONSIDERING THE BOUNDARY CONDITIONS FOR A
DYNAMIC, TRANSIENT MODE I CRACK PROBLEM**

Tanya L. Leise, Jay R. Walton and Yuliya Gorb

Volume 3, N° 9

November 2008

RECONSIDERING THE BOUNDARY CONDITIONS FOR A DYNAMIC, TRANSIENT MODE I CRACK PROBLEM

TANYA L. LEISE, JAY R. WALTON AND YULIYA GORB

A careful examination of a dynamic mode I crack problem leads to the conclusion that the commonly used boundary conditions do not always hold in the case of an applied crack face loading, so that a modification is required to satisfy the equations. In particular, a transient compressive stress wave travels along the crack faces, moving outward from the loading region on the crack face. This does not occur in the quasistatic or steady state problems, and is a special feature of the transient dynamic problem that is important during the time interval immediately following the application of crack face loading. We demonstrate why the usual boundary conditions lead to a prediction of crack face interpenetration, and then examine how to modify the boundary condition for a semi-infinite crack with a cohesive zone. Numerical simulations illustrate the resulting approach.

1. Introductory remarks

The subject of the present contribution is unsteady, dynamic crack propagation in brittle polymers. The subject has received considerable attention in the literature, mostly focused upon experimental and numerical studies with comparatively few results obtained via analytical methods. Analytical solutions to select canonical fracture boundary value problems have an important role to play in gaining a deep understanding of the physical processes involved in dynamic fracture of polymeric materials and their numerical simulation. However, constructing analytical solutions to such boundary values, even subject to various simplifying idealizations, presents many technical obstacles.

There is a growing literature devoted to constructing analytical solutions to dynamic fracture boundary value problems in the context of either linear elasticity or viscoelasticity. Broberg [1999] and Freund [1990] give extensive accounts of these developments prior to 2000. Analytical solutions for dynamic steady (constant crack speed) crack growth in linear viscoelastic materials have been constructed for both mode III (antiplane shear) [Herrmann and Walton 1989; Walton 1987] and mode I (planar opening) [Walton 1990; Herrmann and Walton 1994] fracture conditions.

For dynamic, unsteady crack growth, the catalog of analytical solutions in the literature is much smaller, and almost entirely confined to mode III cracks in elastic material, two exceptions being a paper by Saraikin and Slepyan [1979], which points the way to solving dynamically accelerating mode I cracks in elastic material but does not explicitly exhibit a full solution for general loading, and those by Walton and Leise [2003; 2004] which consider a mode III accelerating crack in a linear viscoelastic material.

Keywords: transient fracture analysis, opening mode crack, boundary conditions, Dirichlet-to-Neumann map.

This work was supported in part by the Army Research Laboratory under contract number W911NF-04-2-00-11 and in part by award number KUS-C1-016-04 made by King Abdullah University of Science and Technology (KAUST).

A number of analytical solutions for dynamic, accelerating mode III crack problems in the setting of linear elasticity have been constructed, both without a cohesive zone [Walton and Herrmann 1992; Leise and Walton 2001b; 2001a] and with a cohesive zone [Costanzo and Walton 1997; 1998]. The subject of the present contribution is to generalize this work to the setting of mode I fracture with a cohesive zone exhibiting nonlinear constitutive behavior modeling an infinitesimally thin evolving craze field in front of an accelerating crack tip. In future work, we will show how this approach can be generalized to a cohesive zone with nonlinear, time dependent constitutive behavior.

2. Mode I crack problem

Consider an infinite, isotropic, homogeneous elastic body with a planar crack along the xz -plane for $x < \ell(t)$ under mode I conditions, where $x = \ell(t)$ locates the crack tip. We can reduce the problem to the xy -plane since the displacement and stress are independent of z , and we can restrict attention to the upper half-plane $y > 0$ if we apply a crack face loading symmetric with respect to the xz -plane. The goal is to determine the crack face displacement due to a time-dependent loading, which we accomplish by adapting the method of Saraikin and Slepyan [1979; 2002] to obtain a boundary integral equation relating the stress and displacement along the x -axis for $t > 0$.

Let $u_k(x, y, t)$ denote the displacement and $\sigma_{ij}(x, y, t)$ the components of the Cauchy stress tensor. The equations of motion in the context of plane strain are

$$\begin{aligned}\rho\ddot{u}_1 &= (2\mu + \lambda)u_{1,11} + \mu u_{1,22} + (\mu + \lambda)u_{2,12}, \\ \rho\ddot{u}_2 &= (2\mu + \lambda)u_{2,22} + \mu u_{2,11} + (\mu + \lambda)u_{1,12},\end{aligned}$$

while the relevant constitutive relations are

$$\sigma_{12} = \mu(u_{1,2} + u_{2,1}), \quad \sigma_{22} = \lambda u_{1,1} + (2\mu + \lambda)u_{2,2}.$$

The initial conditions are

$$u_i(x, y, 0) = 0 \quad \text{and} \quad \dot{u}_i(x, y, 0) = 0,$$

and we assume $\sigma_{ij} \rightarrow 0$ as $x^2 + y^2 \rightarrow \infty$. The mode I assumption is that $\sigma_{12}(x, 0, t) = 0$, for all x and t . The classical crack problem assumes a known loading on the crack faces:

$$\sigma_{22}(x, 0, t) = \Lambda(x, t) \quad \text{for } x < \ell(t).$$

Note that this implies that off the support of $\Lambda(x, t)$, the crack faces are stress free.

The classical crack tip model has $u_2(x, 0, t) = 0$ for $x > \ell(t)$ and a square root singularity in the stress σ_{22} at the crack tip. Alternatively, one can insert a cohesive zone to the right of the crack tip and impose a law such as $\sigma_{22}(x, 0, t) = F(u_2(x, 0, t))$ in the cohesive zone (thereby eliminating the crack tip singularity in the stress). One can then use a critical crack opening displacement criterion to determine the crack tip position: when the displacement at the edge of the cohesive zone reaches the critical value δ_c , the material can no longer support stress and the crack extends. The function F should then satisfy $F(u) \geq 0$, $F(0) = 0$, and $F(\delta_c) = 0$.

We show below that this classical crack model (whether a sharp crack model or a cohesive zone model) can exhibit a logical inconsistency by predicting crack surface interpenetration.

3. Integral equation derivation

Defining Fourier and Laplace transforms (as used in [Saraikin and Slepyan 1979]) via

$$\hat{f}(p, y, t) = \int_{-\infty}^{\infty} e^{ipx} f(x, y, t) dx,$$

$$\hat{f}(p, y, s) = \int_0^{\infty} e^{-st} \hat{f}(p, y, t) dt,$$

the transformed equations of motion become (assuming the initial conditions of $u_k(x, y, 0) = 0$ and $\dot{u}_k(x, y, 0) = 0$ for $k = 1, 2$)

$$\rho s^2 \hat{u}_1 = -p^2(2\mu + \lambda) \hat{u}_1 + \mu \frac{\partial^2}{\partial y^2} \hat{u}_1 - ip(\mu + \lambda) \frac{\partial}{\partial y} \hat{u}_2, \tag{3-1}$$

$$\rho s^2 \hat{u}_2 = (2\mu + \lambda) \frac{\partial^2}{\partial y^2} \hat{u}_2 - p^2 \mu \hat{u}_2 - ip(\mu + \lambda) \frac{\partial}{\partial y} \hat{u}_1, \tag{3-2}$$

and the constitutive relations become

$$\hat{\sigma}_{12} = \mu \left(\frac{\partial}{\partial y} \hat{u}_1 - ip \hat{u}_2 \right), \tag{3-3}$$

$$\hat{\sigma}_{22} = -ip\lambda \hat{u}_1 + (2\mu + \lambda) \frac{\partial}{\partial y} \hat{u}_2. \tag{3-4}$$

The general solutions of equations (3-1) and (3-2) that vanish as $y \rightarrow \infty$ are

$$\hat{u}_1 = A_1(p, s) e^{-\alpha(p,s)y} + B_1(p, s) e^{-\beta(p,s)y}, \tag{3-5}$$

$$\hat{u}_2 = A_2(p, s) e^{-\alpha(p,s)y} + B_2(p, s) e^{-\beta(p,s)y}, \tag{3-6}$$

where $\alpha A_1 = ipA_2$, $-ipB_1 = \beta B_2$, and

$$\alpha(p, s) = \sqrt{p^2 + s^2/c_L^2},$$

$$\beta(p, s) = \sqrt{p^2 + s^2/c_S^2}.$$

Here

$$c_L = \sqrt{\frac{2\mu + \lambda}{\rho}}$$

is the longitudinal wave speed and $c_S = \sqrt{\mu/\rho}$ is the shear wave speed. The functions $\alpha(p, s)$ and $\beta(p, s)$ are decomposed into square roots of linear functions, e.g., $\alpha(p, s) = \sqrt{ip + s/c_L} \sqrt{-ip + s/c_L}$, taken with positive real part (branch cut for $\sqrt{\zeta}$ is taken along negative real axis in the z -plane). Substituting (3-5)–(3-6) into (3-3)–(3-4) and taking the limit $y \rightarrow 0$ yields

$$\hat{\sigma}_{12}(p, 0, s) = \frac{\rho s^2 \alpha(p, s)}{p^2 - \alpha(p, s)\beta(p, s)} \hat{u}_1(p, 0, s) - ip \left(2\mu + \frac{\rho s^2}{p^2 - \alpha(p, s)\beta(p, s)} \right) \hat{u}_2(p, 0, s),$$

$$\hat{\sigma}_{22}(p, 0, s) = ip \left(2\mu + \frac{\rho s^2}{p^2 - \alpha(p, s)\beta(p, s)} \right) \hat{u}_1(p, 0, s) + \frac{\rho s^2 \beta(p, s)}{p^2 - \alpha(p, s)\beta(p, s)} \hat{u}_2(p, 0, s).$$

The plane strain problem can be simplified to a single equation by assuming that there is no shear surface traction, $\sigma_{12}(x, 0, t) = 0$ for all x . This assumption leads to the relation

$$\hat{\sigma}(p, s) = \frac{\mu^2 R(p, s)}{\rho s^2 \alpha(p, s)} \hat{u}(p, s), \tag{3-7}$$

where $\sigma(x, t) = \sigma_{22}(x, 0, t)$ and $u(x, t) = u_2(x, 0, t)$. The Rayleigh function $R(p, s)$ is defined by

$$R(p, s) = 4p^2 \alpha(p, s) \beta(p, s) - (2p^2 + s^2/c_s^2)^2.$$

Note that the Rayleigh function $R(p, s)$ has zeros only at $p = \pm is/c_R$. Define the transfer function \hat{S} to be

$$\hat{S}(p, s) = \frac{\rho s^2 \alpha(p, s)}{\mu^2 R(p, s)},$$

and let $\hat{P} = 1/\hat{S}$. These transfer functions can be decomposed as

$$\hat{P}(p, s) = \hat{P}_+(p, s) \hat{P}_-(p, s) \quad \text{and} \quad \hat{S}(p, s) = \hat{S}_+(p, s) \hat{S}_-(p, s)$$

in such a manner that the functions $S_{\pm}(x, t)$ and $P_{\pm}(x, t)$ satisfy the following conditions:

$$S_+(x, t) = P_+(x, t) = 0 \quad \text{whenever } x > c_L t \text{ or } x < 0, \tag{3-8}$$

$$S_-(x, t) = P_-(x, t) = 0 \quad \text{whenever } x < -c_L t \text{ or } x > 0. \tag{3-9}$$

This leads to the integral equation (as derived in [Saraikin and Slepyan 1979]):

$$S_+ ** \sigma = P_- ** u, \tag{3-10}$$

where double asterisks refer to convolution with respect to both x and t :

$$f ** g(x, t) = \int_0^t \int_{-\infty}^{\infty} f(x - r, t - s) g(r, s) dr ds.$$

We use a slightly different factorization than [Saraikin and Slepyan 1979] (in which the goal was to restrict the support of these functions in order to derive the stress intensity factor). The original decomposition in [Saraikin and Slepyan 1979] and the one given below differ only by a factor of s , effectively removing a time derivative from the expression for S_+ and thereby easing numerical computations involving that function. We do not need the stress intensity factor here, since we consider a cohesive zone, so the changes to the support properties of S_{\pm} due to this slight difference do not pose a difficulty for us. This small alteration to the factorization is solely to reduce the complexity of the computations of the stress and displacement expressions (which involve convolutions with S_+ and a related function T_- defined below).

We decompose the transfer function $\hat{S}(p, s)$ as follows:

$$\hat{S}_+ = \frac{\sqrt{as - ip}}{s(cs - ip)} D_+(ip/s), \quad \hat{S}_- = -\frac{b^2 s \sqrt{as + ip}}{2\mu(b^2 - a^2)(cs + ip)} D_-(ip/s),$$

where $a = \frac{1}{c_L}$, $b = \frac{1}{c_S}$, $c = \frac{1}{c_R}$, and

$$D_{\pm}(ip/s) = 1 + \int_a^b \frac{F_1(u)du}{u \mp ip/s}, \quad F_1(u) = \gamma(u) \exp[\aleph(u)],$$

$$\gamma(u) = \frac{4}{\pi} \frac{u^2 \sqrt{b^2 - u^2} \sqrt{u^2 - a^2}}{\sqrt{(b^2 - 2u^2)^4 + 16u^4(b^2 - u^2)(u^2 - a^2)}}, \quad \aleph(u) = \frac{1}{\pi} P.V. \int_a^b \varphi(\alpha) \frac{d\alpha}{\alpha - u},$$

$$\varphi(\alpha) = \tan^{-1} \frac{4\alpha^2 \sqrt{b^2 - \alpha^2} \sqrt{\alpha^2 - a^2}}{(b^2 - 2\alpha^2)^2} = \sin^{-1} \frac{4\alpha^2 \sqrt{b^2 - \alpha^2} \sqrt{\alpha^2 - a^2}}{\sqrt{(b^2 - 2\alpha^2)^4 + 16\alpha^4(b^2 - \alpha^2)(\alpha^2 - a^2)}}.$$

The reciprocal of $D_{\pm}(ip/s)$ is given by

$$D_{\pm}^{-1}(ip/s) = 1 + \int_a^b \frac{F_2(u)du}{u \mp ip/s}, \quad \text{where } F_2(u) = -\gamma(u) \exp[-\aleph(u)].$$

4. Crack face interpenetration

We now carefully examine the integral equation $S_+ ** \sigma = T_- ** Du = D(T_- ** u)$, where T_- is defined as

$$P_- = D \circ T_- \quad \text{and} \quad D = \left(c \frac{\partial}{\partial t} - \frac{\partial}{\partial x} \right).$$

Examination of the functions S_+ and T_- yields some unexpected results. The basic definitions are

$$\begin{aligned} G_1(s) &= 1 - H(b-s) \int_s^b F_1(u) \sqrt{\frac{u-a}{u-s}} \frac{du}{c-u}, \\ G_2(s) &= 1 + H(b-s) \int_s^b F_2(u) \frac{du}{\sqrt{u-a} \sqrt{u-s}}, \\ S_+(x, t) &= \frac{H(x)}{\sqrt{\pi x}} H(t-ax) \left[G_1(t/x) - H(c-t/x) B \sqrt{\frac{c-a}{c-t/x}} \right], \\ T_-(x, t) &= -\frac{2\mu(b^2 - a^2)}{b^2} \left[\frac{H(-x)}{\sqrt{-\pi x}} H(t+ax) G_2(-t/x) \right], \end{aligned} \tag{4-1}$$

where

$$B = G_1(a) = 1 - \int_a^b F_1(u) \frac{du}{c-u}.$$

See Figures 1 and 2 for graphs of $G_1(s) - H(c-s) B \sqrt{(c-a)/(c-s)}$ and $G_2(s)$.

Suppose $(b/a)^2 \geq 2$, corresponding to a nonnegative Poisson ratio λ . The numerical results shown in Figures 1 and 2 indicate that the function $T_-(x, t)$ is always negative for $-c_L t < x < 0$, while $S_+(x, t)$ changes sign: $S_+(x, t) < 0$ for $c_R t < x < c_L t$, $\lim_{t/x \rightarrow c^-} S_+(x, t) = -\infty$ due to the term involving $1/\sqrt{c-t/x}$, and $S_+(x, t) > 0$ for $0 < x < c_R t$.

Consider the following scenario. Suppose the loading $\sigma_-(x, t) = \Lambda(x, t)$ has support on a fixed interval $(-d-L, -d)$, on which it is always negative, and further suppose that the cohesive zone has

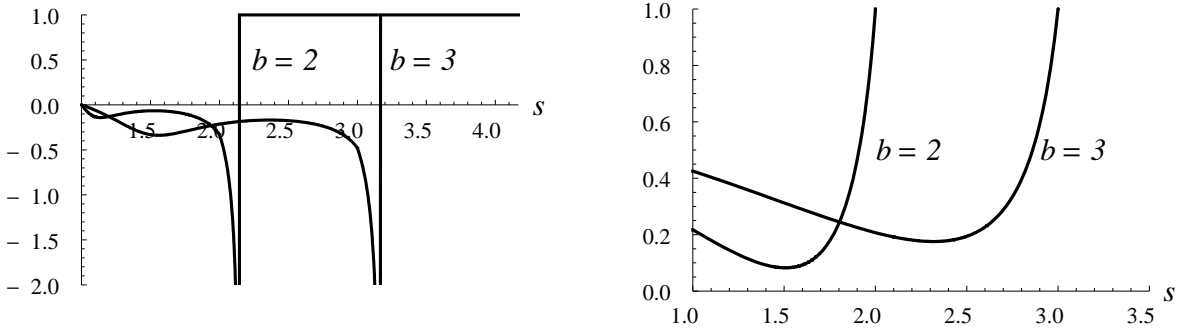


Figure 1. Graph of $G_1(s) - H(c - s)B\sqrt{(c - a)/(c - s)}$ on the left and of $G_2(s)$ on the right for $a = 1$, $b = 2.0, 3.0$, and $c \approx 2.14, 3.17$, respectively. The function $G_1(s) - H(c - s)B\sqrt{(c - a)/(c - s)}$ involves a square root singularity and sign switch at $s = c = 1/c_R$, while $G_2(s)$ is always positive.

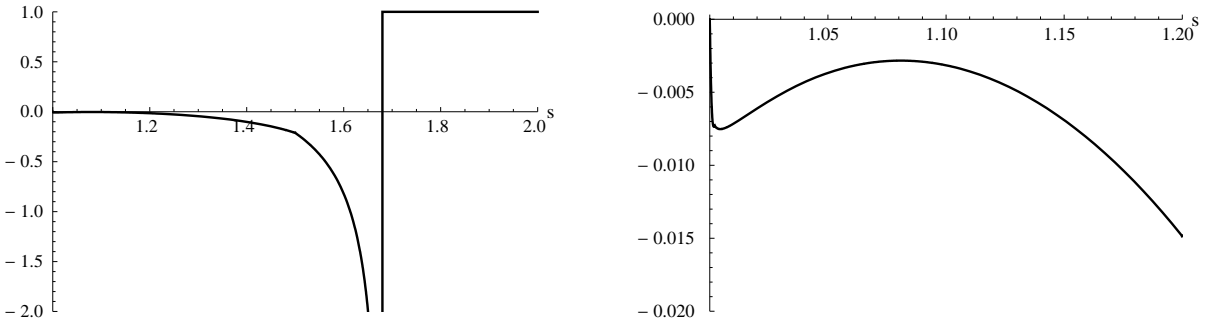


Figure 2. Graphs of $G_1(s) - H(c - s)B\sqrt{(c - a)/(c - s)}$ for $a = 1$, $b = 1.5$, and $c \approx 1.68$, showing that even for values of b close to $a\sqrt{2}$ this function remains negative on the interval (a, c) .

not yet begun opening (implying zero stress on the unloaded crack faces and to the right of the crack tip). Let R be the region in the xt -plane defined by

$$-d + c_R t < x < -d + c_L t \quad \text{and} \quad t > 0.$$

If $(x, t) \in R$, then S_+ is negative on the domain involved in the convolution $(S_+ ** \Lambda)(x, t)$ and so this convolution will be positive. See Figure 3. The integral equation relating stress and displacement is

$$S_+ ** \Lambda = D(T_- ** u);$$

integrate both sides with respect to Rayleigh characteristic to remove the derivative D . If $(x, t) \in R$, then this integral is along a line segment contained within R . Hence the integral of $S_+ ** \sigma$ will be positive if $(x, t) \in R$. Since T_- is nonpositive, the integral equation implies that the displacement must be negative on some portion of the crack face. See Figure 4 for a simulation showing that this negative displacement appears in the context of a cohesive zone as well.

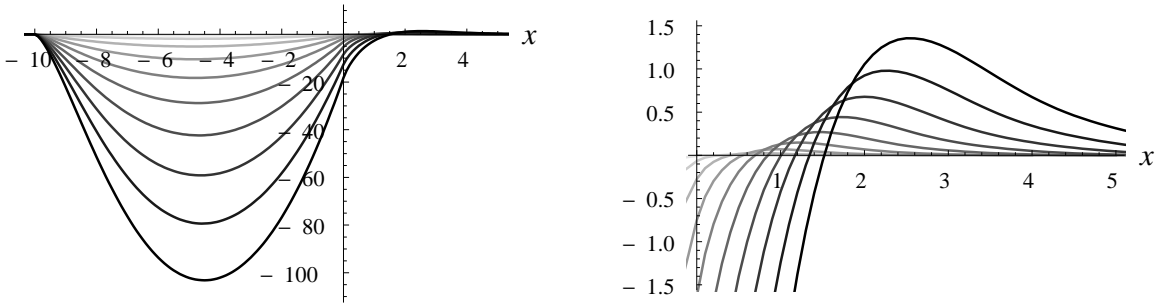


Figure 3. Graph of $S_+(x, t)$ convolved with the loading (with $L = 10$) on the crack face, where $b = 2$. Profiles of $(S_+ ** \Lambda)(x, t)$ are shown for times $t = 1, 2, \dots, 10$ (in dimensionless units). This convolution is usually negative, but at the extreme right is positive, as only the region where S_+ is negative is involved in the convolution for these values.

5. Implications

This reasoning implies that we cannot assume zero stress on the unloaded (“free”) portion of the crack faces. This would mean that other solution methods for mode I fracture that explicitly assume zero stress on the unloaded portion of the crack faces are also missing the small compressive stress occurring behind the longitudinal wave front. That is, we are not free to specify *a priori* the stress on the entire crack face and the parts of the boundary where displacement is zero, contrary to common assumption.

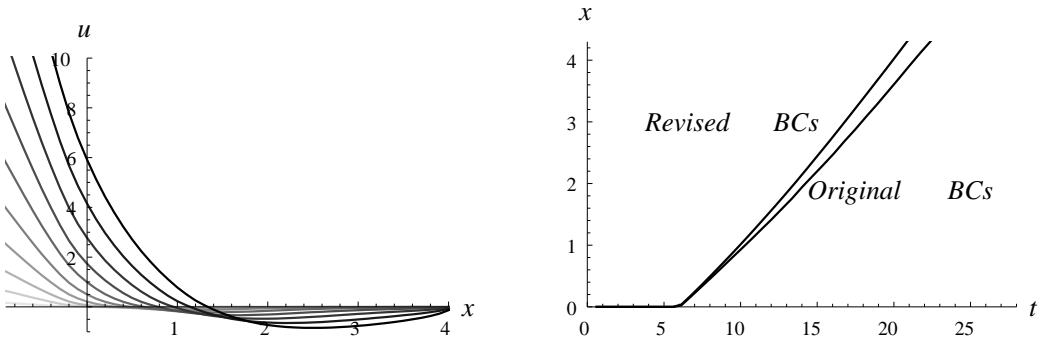


Figure 4. Example with $b = 2$, showing negative displacements from integral equation calculations under the assumption that the unloaded crack faces and the region to the right of the cohesive zone will be stress-free. The graph on the left shows the displacement profiles at times $t = 1, 2, \dots, 10$ (in dimensionless units), where the crack tip begins accelerating at $t \approx 6.1$. While these negative displacements are very small compared to those in the loading interval, they do have a significant effect in preventing the crack faces from properly opening and so significantly impact transient crack tip calculations, as shown in the graph on the right of the crack tip position $x = \ell(t)$.

If the loading is changing — cycling, for example — the resulting boundary values could be quite complicated and involve multiple regions where the stress must be computed. The problem becomes similar to a crack closure problem, for which stresses on the crack faces must be computed.

6. Modification of the boundary conditions

Since negative displacement doesn't make physical sense, the boundary conditions must be modified. We can't assume that the stress is always zero on the part of the crack face where the applied load is zero (or in the region to the right of a cohesive zone). There can be a small compressive stress traveling at the longitudinal wave speed that must be calculated as part of the solution (as depicted in Figure 5). Perhaps this is due to the point on the crack face where the displacement first equals zero acting as a pivot: the crack face to the left of the pivot is pushed up and so the crack face to the right tends to be pressed down. This compressive stress wave will continue along the boundary, moving out from the applied loading interval in both positive and negative directions.

Consider the integral equation (3-10) in the case that the loading increases in strength over time on a loading interval $[-d - L, -d]$, where the right end is a nonzero distance from the crack tip. Let $\Lambda(x, t)$ represent the crack face loading and u_- the crack face displacement. Let u_+ represent the cohesive zone displacement, so that $\sigma_+ = F(u_+)$ is the cohesive stress. Regions of compressive stress will travel out from the left and right edges of the loading interval on the crack face with speed c_L . Let the curve $x = r(t)$ mark the front edge of the region of compressive stress traveling to the right; this also marks where the displacement becomes zero. Note that $r(0) = -d < \ell(0)$, so $x = r(t)$ begins to the left of the crack tip path $x = \ell(t)$ and typically crosses it. Let σ_r represent the stress in the region $r(t) < x < c_L t$. For $x > -d - L$, the integral equation (3-10) expands to

$$S_+ ** F(u_+) + S_+ ** \sigma_r + S_+ ** \Lambda = P_- ** u_+ + P_- ** u_- \tag{6-1}$$

This can be used to solve for the displacements u_+ and u_- . We also need to calculate σ_r . Fortunately,

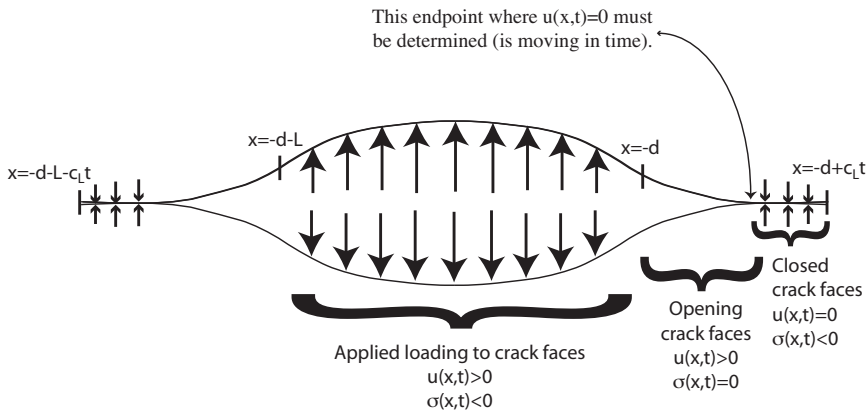


Figure 5. New scheme with a compressive stress in front of the opening portion of the crack faces. The curve $x = r(t)$ where the opening displacement becomes zero and the compressive stresses for $x > r(t)$ must be determined.

the $T_{-} ** u_{\pm}$ terms in this case drop out, so the integral equation reduces to

$$S_{+} ** \sigma_r = -S_{+} ** F(u_{+}) - S_{+} ** \Lambda, \tag{6-2}$$

for $x > r(t)$.

7. Numerical methods

We discretize using a grid in characteristic coordinates $\eta = t + ax$ and $\zeta = t - ax$, after nondimensionalizing the integral equations (length with respect to δ_c , time with respect to $a\delta_c$, and stress with respect to μ , where δ_c is the critical crack opening displacement). In the simulations shown in the figures, we implicitly refer to the dimensionless slownesses $a = 1$, $b = c_L/c_S$, and $c = c_L/c_R$. We use continuous piecewise linear approximations of the displacement (using triangles) and continuous piecewise quadratic approximations of the stress on quadrilaterals. This is compatible with the various convolution domains, including on the crack face and in the cohesive zone.

The basic process is to step with respect to increasing values of ζ . For each ζ value, we find nodal values of the displacement and stress for increasing values of η on the grid. There are three cases:

- (1) Solve (6-1) for $u_{-}(x, t)$ if $x < \min\{\ell(t), r(t)\}$.
- (2) Solve (6-1) for $u_{+}(x, t)$ if $\ell(t) < x < r(t)$.
- (3) Solve (6-2) for $\sigma_r(x, t)$ if $r(t) < x < c_L t$.

In each case, all the required values in the integral equation will be known from previous steps.

The computations are done efficiently by precomputing all needed convolutions on two prototype triangles and a quadrilateral. These can then be used repeatedly to avoid redundant integrations. These precomputed convolution values scale with the step size, so this lengthy set of computations only needs to be done once.

For examples of simulations, see Figures 6 and 7. In these examples, $\Lambda(x, t) = 0.08t(x+d)(x+d+L)$ on $[-d-L, -d]$ and equals zero otherwise, where $d = 0.2$ and $L = 10$ (all in dimensionless units). The

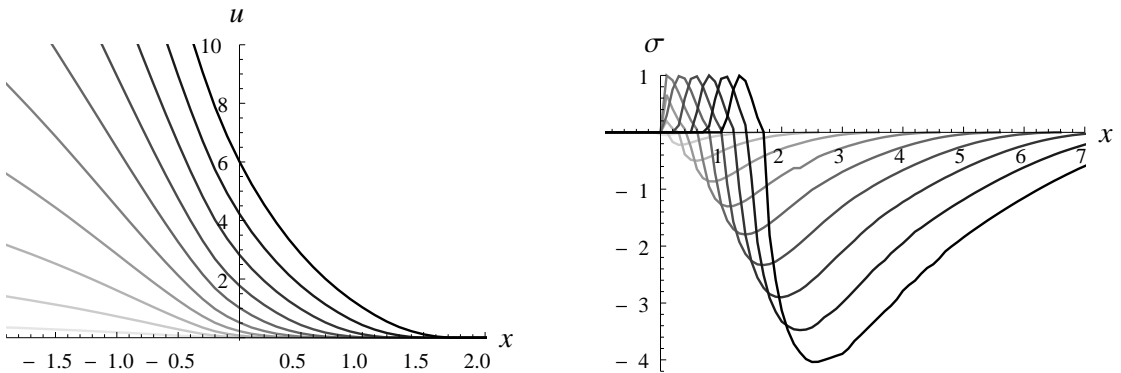


Figure 6. Example of a simulation using the revised scheme. Profiles of the displacement u and stress σ for times $t = 1, 2, \dots, 10$, all in dimensionless units. See Section 7 for modeling details. The stress equals zero at the crack tip, is positive within the cohesive zone, and negative in the region to the right of the cohesive zone.

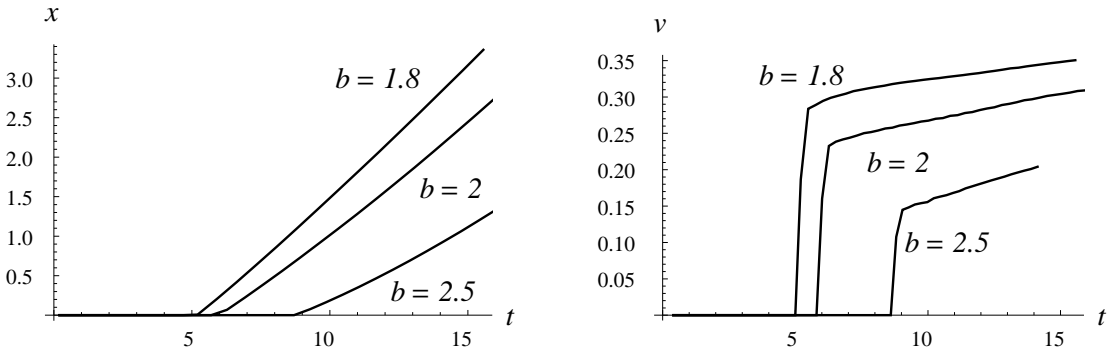


Figure 7. Comparison of crack tip paths and speeds for different ratios $b = c_L/c_S$, using dimensionless units.

crack tip is initially located at $x = 0$, and begins to run once the opening displacement equals 1 at the crack tip position (which is the left edge of the cohesive zone). The crack propagates according to a critical crack opening displacement criterion. The cohesive zone law in dimensionless units is $F(u) = 6.75u(1 - u)^2$ (maximum cohesive stress equals 1). The right edge path $r(t)$ is determined by calculating the value of η at which the displacement will first equal zero for the current value of ζ . We use step size $\Delta\zeta = \Delta\eta = 0.1$ in all simulations.

8. Concluding remarks

The problem considered is that of the unsteady, dynamic propagation of a semi-infinite, pure mode I crack in a brittle polymer. The bulk material is modeled as an infinite, homogeneous, isotropic linearly elastic body with a crack with a cohesive zone ahead of the advancing crack tip. The cohesive zone constitutive behavior is modeled through a nonlinear elastic-like response relation incorporating an evolving damage parameter. It was shown that the classical crack paradigm that assumes zero stress outside the loading interval and cohesive zone must be modified in this unsteady, dynamic mode I setting since it predicts zones of crack face interpenetration in a neighborhood of the crack tip (Figure 4). Consequently, the classical crack/cohesive zone model must be generalized to include a contact/slip zone between the fully opened crack and the cohesive zone (Figure 5). The extent of the contact/slip zone must be determined as part of the boundary value problem solution by imposition of the requirement that the displacement discontinuity across the fracture plane (the crack opening displacement) must be everywhere nonnegative. This effect is not seen in dynamic steady-state or transient quasistatic analyses or in the transient dynamic mode III case; it follows from properties of the Dirichlet-to-Neumann map appropriate for transient, dynamic mode I fracture problems.

References

[Broberg 1999] K. B. Broberg, *Cracks and fracture*, Academic Press, San Diego, CA, 1999.
 [Costanzo and Walton 1997] F. Costanzo and J. R. Walton, "A study of dynamic crack growth in elastic materials using a cohesive zone model", *Int. J. Eng. Sci.* **35**:12-13 (1997), 1085–1114.

- [Costanzo and Walton 1998] F. Costanzo and J. R. Walton, “Numerical simulations of a dynamically propagating crack with a nonlinear cohesive zone”, *Int. J. Fract.* **91**:4 (1998), 373–389.
- [Freund 1990] L. B. Freund, *Dynamic fracture mechanics*, Cambridge, Cambridge, 1990.
- [Herrmann and Walton 1989] J. M. Herrmann and J. R. Walton, “On the energy release rate for dynamic transient anti-plane shear crack propagation in a general linear viscoelastic body”, *J. Mech. Phys. Solids* **37**:5 (1989), 619–645.
- [Herrmann and Walton 1994] J. M. Herrmann and J. R. Walton, “The energy release rate for transient dynamic mode I crack propagation in a general linearly viscoelastic body”, *Quart. Appl. Math.* **52**:2 (1994), 201–228.
- [Leise and Walton 2001a] T. L. Leise and J. R. Walton, “A general method for solving dynamically accelerating multiple co-linear cracks”, *Int. J. Fract.* **111**:1 (2001), 1–16.
- [Leise and Walton 2001b] T. L. Leise and J. R. Walton, “Dynamically accelerating cracks, II: A finite length mode III crack in elastic material”, *Quart. Appl. Math.* **59**:4 (2001), 601–614.
- [Leise and Walton 2004] T. L. Leise and J. R. Walton, “An analytical and numerical study of a dynamically accelerating semi-infinite crack in a linear viscoelastic material”, *Int. J. Fract.* **127**:2 (2004), 101–117.
- [Saraikin and Slepyan 1979] V. A. Saraikin and L. I. Slepyan, “Plane problem of the dynamics of a crack in an elastic solid”, *Mech. Solids* **14**:4 (1979), 46–62.
- [Slepyan 2002] L. I. Slepyan, *Models and phenomena in fracture mechanics*, Springer, Berlin, 2002.
- [Walton 1987] J. R. Walton, “The dynamic, energy release rate for a steadily propagating anti-plane shear crack in a linearly viscoelastic body”, *J. Appl. Mech. (ASME)* **54**:3 (1987), 635–641.
- [Walton 1990] J. R. Walton, “The dynamic energy release rate for a steadily propagating mode I crack in an infinite, linearly viscoelastic body”, *J. Appl. Mech. (ASME)* **57**:2 (1990), 343–353.
- [Walton and Herrmann 1992] J. R. Walton and J. M. Herrmann, “A new method for solving dynamically accelerating crack problems, I: The case of a semi-infinite mode III crack in elastic material revisited”, *Quart. Appl. Math.* **50**:2 (1992), 373–387.
- [Walton and Leise 2003] J. R. Walton and T. L. Leise, “A method for solving dynamically accelerating crack problems in linear viscoelasticity”, *SIAM J. Appl. Math.* **64**:1 (2003), 94–107.

Received 4 Sep 2008. Revised 18 Nov 2008. Accepted 20 Nov 2008.

TANYA L. LEISE: tleise@amherst.edu

Amherst College, Department of Mathematics and Computer Science, Amherst, MA 01002, United States

JAY R. WALTON: jwalton@math.tamu.edu

Texas A & M University, Department of Mathematics, College Station, TX 77843-3368, United States

YULIYA GORB: gorb@math.tamu.edu

Texas A & M University, Department of Mathematics, College Station, TX 77843-3368, United States

